Antimonide-based 2.3 [micro sign]m photonic crystal coupled-cavity lasers for CH4 QEPAS

Mohammad Jahjah, Souad Moumdji, Olivier Gauthier-Lafaye, S. Bonnefont, Yves Rouillard, Aurore Vicet

Antimonide-based 2.3 mm photonic crystal coupled-cavity lasers for CH_4 QEPAS

M. Jahjah, S. Moumdji, O. Gauthier-Lafaye, S. Bonnefont, Y. Rouillard and A. Vicet

GaInAsSb/AlGaAsSb quantum wells lasers have been grown by molecular beam epitaxy and processed into ridge cavities coupled by an intracavity photonic crystal mirror. The lasers operate at room tempera-ture in the continuous wave regime at 2.35 μm. One of these devices was used as an excitation source on a methane sensor based on quartz-enhanced photoacoustic spectroscopy. A spectrophone, consist-ing of a quartz tuning fork and two steel microresonators, was used. A detection limit of 400 ppbv was achieved using second derivative wavelength modulation detection.

Introduction: This Letter presents a semiconductor laser to be used in a methane optical sensor based on a quartz enhanced photoacoustic spectroscopy (QEPAS) spectrophone. Natural gas is the energy source having undergone the steepest growth in the last 30 years: the demand has doubled since 1980. Such a rise is accompanied by an equivalent need for efficient leak detectors along gas pipes. In a quite different connection, atmospheric methane raised concerns in the early 2000s for environmental reasons and has become one of the recommended key atmospheric gases [1] to be measured by GAW (Global Atmosphere Watch).

Tunable diode laser spectroscopy requires tunable light sources exhibiting a single-frequency emission. For a few years, we have worked on new laser sources. They are based on an integrated version of cleaved coupled cavities (C^3), with two cavities separated by an etched photonic crystal (PhC) mirror, providing longitudinal mode selection for stable single-frequency operation. The advantage of this device is that, contrary to C^3 lasers, it is a non-cleaved component. The PhC mirror acts as a cleaved reflecting facet, with a wavelength-controlled response with specifications adjustable by the optical design. The first devices made on GaSb proposed according to this scheme [2] emitted at 1.9 μm. We have adapted the concept to develop the first coupled-cavity PhC (C^2 PhC) devices operating above 2.6 μm [3] with a PhC mirror on both sides of the laser ridge.

In this Letter, we repeat devices emitting at 2.35 μm based on the C^2 PhC concept with an optimised design where the intracavity mirror is fully crossing the laser ridge, to enhance coupling effects between the two cavities. One of these devices has been used in a QEPAS CH_4 sensor [4].

Study and fabrication of photonic-crystal-based antimonide lasers: The laser structure was grown by molecular beam epitaxy in a Varian Gen II system equipped with two valved As and Sb cracker cells. The growth was carried out on an *n*-type (100) GaSb substrate. The temperature was fixed at 480°C. Layers of the structure were grown in the following order: a 75 nm-thick *n*-type GaSb buffer, a 90 nm-thick *n*-type layer graded from $Al_{0.10}Ga_{0.90}As_{0.03}Sb_{0.97}$ to $Al_{0.90}Ga_{0.10}As_{0.07}Sb_{0.93}$, a 1 μm-thick $Al_{0.90}Ga_{0.10}As_{0.07}Sb_{0.93}$ *n*-type (2×10^{18} cm^{-3}, Te) cladding layer, an undoped active zone consisting of two 10 nm-thick quantum wells in $Ga_{0.61}In_{0.39}As_{0.17}Sb_{0.83}$ separated by one 30 nm-thick $Al_{0.25}Ga_{0.75}As_{0.02}Sb_{0.98}$ barrier and enclosed between 370 nm-thick $Al_{0.25}Ga_{0.75}As_{0.02}Sb_{0.98}$ spacers, a 1 μm-thick *p*-type $Al_{0.90}Ga_{0.10}As_{0.07}Sb_{0.93}$ (2×10^{18} cm^{-3}, Be) cladding layer, a 90 nm-thick *p*-type layer graded from $Al_{0.90}Ga_{0.10}As_{0.07}Sb_{0.93}$ to $Al_{0.10}Ga_{0.90}As_{0.03}Sb_{0.97}$ and finally a 300 nm p^+-GaSb cap layer (2×10^{19} cm^{-3}, Be).

A 5 μm-wide ridge waveguide was formed using optical lithography and a Cl_2/N_2 inductively coupled plasma step. The ridge is interrupted to form two laser cavities, separated by a $d = 10$ μm-wide hexagonal photonic crystals lattice. We have used a lattice consisting of holes 350 nm in diameter with a period of 600 nm (filling factor of 30%).

To define the PhC, we use a composite mask made of a 200 nm-thick SiO_2 layer deposited by plasma enhanced chemical vapour deposition topped by a 470 nm-thick layer of polymethylmetacrylate (PMMA). After e-beam exposure, the PMMA is developed and acts as a mask during opening of the SiO_2. The 2D-PhC deep etching process uses this layer as a hard mask. To achieve high aspect ratio deep etching of sub micrometre holes, we use a multi-step etching process combining Cl_2, O_2 and N_2 ICP plasma etching [5].

Finally, the samples were insulated and top contact pads were deposited. They were then thinned down to a thickness of 100 μm before the bottom contact deposition, and cleaved into laser bars. Fig. 1 shows an optical microscope image of the intracavity region with a photonic crystal having two rows of holes.

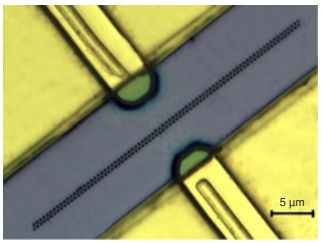

Fig. 1 *Optical microscope image of intracavity region with PhCs crossing ridge waveguide*

Lasers characterisations: The lasers are mounted onto copper heatsinks. We have chosen unbalanced cavity length with 453 μm-long and 1093 μm-long cavities. Two laser configurations can be exploited [6]. In the 'active–passive' configuration, only one of the two cavities is electrically pumped. In the 'active–active' configuration, both cavities are pumped, which leads to a modal selectivity based on the vernier effect operating on the two longitudinal comb-modes: only one mode is selected.

We have two different bias modes of the cavities. In the first, the two cavities are fed with the same current ('short-cut mode'). In the second, different currents are injected into the two cavities. I_S designates the injected current in the short cavity while I_L is that for the long cavity.

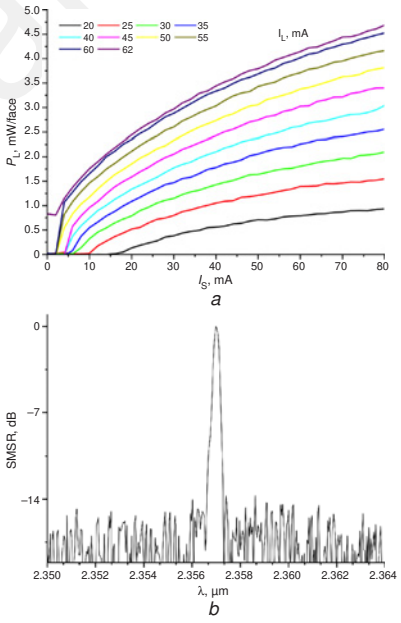

Fig. 2 *Output power characteristics and emission spectrum*

a Output power characteristics of C^2 PhC device with unbalanced cavity lengths against short section current, for different fixed long section currents. For $T = 24$°C, $I_s = 0$ mA, laser emission is obtained for 'quasi-threshold' current of 62 mA

b Emission spectrum at $I_L = 62$ mA, $I_S = 0$ mA, at 24°C, showing sidemode suppression ratio of 14 dB

Fig. 2*a* shows the light–current characteristics of a C^2 PhC laser as a function of current in the short section for various fixed currents injected into the long section. The measured power is emitted by the long cavity. We observe that the quasi-threshold current of the long cavity is strongly dependent on the current feeding the short cavity: it decreases with growing short cavity current. We attribute this behaviour to a decrease of the absorption losses in the short cavity. The emitted power reaches 4.5 mW/facet at $I_S = 80$ mA for $I_L = 60$ mA.

We then studied the injection mode when only the long cavity is fed. In this case, the short cavity is a passive reflector and the lasing mode is filtered by the cavity comb-mode. Fig. 2*b* is an illustration of this

behaviour: one mode is selected, with a sidemode suppression ratio of 14 dB. This low value is explained by a non-sufficient electrical insulation between the two cavities (~100 Ω), due to an accidental oxidation of the upper cladding layer. As a consequence, current leaks from one cavity to another induce a degradation of the modal properties of the device.

Gas sensing: application to CH_4 detection: In QEPAS, a quartz tuning fork (QTF) replaces the microphone used in the standard photoacoustic spectroscopy technique. Its advantages are a high quality factor, small dimensions and low price. This technique has shown high immunity to acoustic noise thanks to the use of the QTF: it has a very narrow frequency response that excludes noise at other frequencies. In this work we used 2*f* detection: the emitted laser beam is modulated at half the QTF resonant frequency ($f = f_0/2$). Once the gas absorbs the optical energy, an acoustic wave is generated: the QTF prongs vibrate owing to their interaction with the wave and a weak current is generated.

The experimental setup consists of a C^2 PhC laser in the 'short-cut' mode, a converging CaF_2 lens and a spectrophone included in the gas cell (details in [7]). The spectrophone consists of two stainless steel tubes placed on both sides of the QTF [8], to enhance the QEPAS signal [4, 7, 8]. The laser temperature is regulated at 22°C and the injected current is generated by a laser driver. A slow frequency current ramp ($f_{ramp} = 0.75$ Hz) is added to the continuous drive current to tune the emitted wavelength. The emitted laser beam is modulated by modulating the current feeding the device. The QTF generated current is converted into a voltage by using a transimpedance amplifier with a 10 MΩ feedback resistor. This signal is demodulated at $f_0 =$ 32738.4 Hz, with a time constant fixed at 100 ms. The signal is then averaged 12 times.

The gas cell is filled with 10 and 2 ppmv of CH_4/N_2. The QEPAS signal shape corresponds to the second derivative of the detected absorption line, and it is proportional to the detected methane concentration (Fig. 3). The detection limit (1σ) of this QEPAS sensor with a C^2 PhC laser is 400 ppbv, reaching the state of the art as far as QEPAS for CH_4 is concerned.

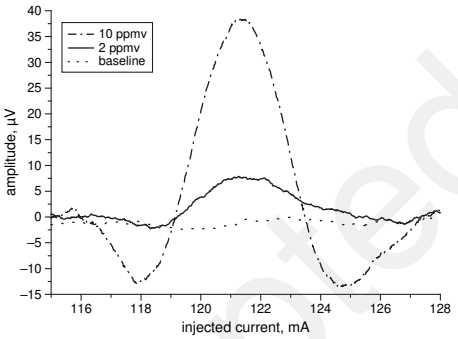

Fig. 3 *2f CH_4 detection of 10 ppmv and 2 ppmv, respectively, and baseline (without gas) measurement*
T = 22°C, f = 16369.2 Hz, ΔI = 4.76 mA

Conclusions: The technological process developed on these laser structures allowed the development of an alternative design of single frequency lasers. Based on the coupled-cavity concept with photonic crystals as intra-cavity mirror, the lasers can be tuned to adjust the emission on strong absorption lines. QEPAS sensing was performed on low concentration CH_4/N_2 gas mixtures to evaluate the detection limit of the system. These results show that the sensor can be very efficient for sensitive trace gas detection around 2.35 μm.

Acknowledgments: We acknowledge the courtesy of our colleague L. Cerutti from IES in providing us with an excellent MBE sample. This work was supported in part by the French National Research Agency (ANR) under Grant ANR-07-BLAN-0326-01, the French Environment and Energy Management Agency (ADEME) and the Languedoc-Roussillon region.

11 December 2011
doi: 10.1049/el.2011.3614
One or more of the Figures in this Letter are available in colour online.

M. Jahjah, S. Moumdji, Y. Rouillard and A. Vicet (*IES, UMR CNRS 5214, CC067, Université Montpellier 2, Place Eugène Bataillon, 34095 Montpellier cedex 05 –France*)

E-mail: a.vicet@univ-montp2.fr

O. Gauthier-Lafaye and S. Bonnefont (*CNRS, LAAS, 7 avenue du colonel Roche Université de Toulouse UPS, INSA, INP, ISAE; LAAS; F-31077 Toulouse, France, Toulouse F-31077, France*)

References

1 WMO 2007, 'WMO Global Atmosphere Watch (GAW) Strategic Plan (2008–2015)', GAW Report No. 172 (WMO TD NO. 1384), World Meteorological Organization, Geneva, Switzerland, 2008
2 Muller, M., Scherer, H., Lehnhardt, T., Rossner, K., Hummer, M., Werner, R., and Forchel, A.: 'Widely tunable coupled cavity lasers at 1.9 μm on GaSb', *IEEE Photonics Technol. Lett*, 2007, **19**, (8), pp. 592–594
3 Moumdji, S., Larrue, A., Belharet, D., Dubreuil, P., Bonnefont, S., Gauthier-Lafaye, O., Rouillard, Y., and Vicet, A.: '2.6 mm GaSb based photonic crystal coupled cavity lasers', *Electron. Lett.*, 2009, **45**, (22), pp. 1119–1121
4 Kosterev, A.A., Bakhirkin, Y.A., Curl, R.F., and Tittel, F.K.: 'Quartz-enhanced photoacoustic spectroscopy', *Opt. Lett*, 2002, **27**, pp. 1902–1904
5 Larrue, A., Moumdji, S., Belharet, D., Dubreuil, P., Bonnefont, S., Gauthier-Lafaye, O., Monmayrant, A., and Lozes-Dupuy, F.: 'ICP etching of high aspect ratio 2D photonic crystals in Al-rich AlGaAs and AlGaAsSb', *J. Vac. Sci. Technol. B*, 2011, **29**, p. 021006
6 Coldren, L.A., Furuya, K., Miller, B.I., and Rentschler, J.A.: 'Etched mirror and groove – coupled GaInAsP/InP laser devices for integrated optics', *IEEE J. Quantum Electron.*, 1982, **QE-18**, (10), pp. 1667–1676
7 Jahjah, M., Vicet, A., and Rouillard, Y.: 'A QEPAS based methane sensor with a 2.35 μm antimonide laser', *Appl. Phys. B*, 2011 DOI 10.1007/s00340-011-4671-4
8 Dong, L., Kosterev, A.A., Thomazy, D., and Tittel, F.K.: 'QEPAS spectrophones: design, optimization, and performance', *Appl. Phys. B*, 2010, **100**, pp. 627–635